

文章编号: 1006-9941(2008)06-0663-06

## Preparation Crystal Structure and Thermal Decomposition Mechanism of $\text{Mn}(\text{CHZ})_2(\text{N}_3)_2$

LIU Zhen-hua, ZHANG Tong-lai, ZHANG Jian-guo, YANG Li, ZHANG Jin, ZANG Yan

(State Key Laboratory of Explosion Science and Technology, Beijing Institute of Technology, Beijing 100081, China)

**Abstract:** A mixed ligand complex of manganese(II) carbohydrazide azide,  $\text{Mn}(\text{CHZ})_2(\text{N}_3)_2$  (CHZ = carbohydrazide), was synthesized and characterized by using elemental analysis and Fourier transform infrared (FT-IR) spectrum. Its crystal structure was determined by single crystal X-ray diffraction analysis. The crystal belongs to triclinic,  $P\bar{1}$  space group,  $a = 8.2217(17) \text{ \AA}$ ,  $b = 8.7427(18) \text{ \AA}$ ,  $c = 9.4532(19) \text{ \AA}$ ,  $\alpha = 86.376(4)^\circ$ ,  $\beta = 69.104(3)^\circ$ ,  $\gamma = 74.019(3)^\circ$ ,  $V = 609.8(2) \text{ \AA}^3$ ,  $D_c = 1.738 \text{ g} \cdot \text{cm}^{-3}$ ,  $Z = 2$ ,  $R_1 = 0.0316$ ,  $wR_2[I > 2\sigma(I)] = 0.0826$  and  $S = 1.132$ . The central Mn(II) ion is six-coordinated with two carbohydrazide molecules and two monodentate azido ligands, and carbohydrazide serves as bidentate ligands through the carbonyl oxygen atom and one of the terminal nitrogen atoms. The thermal decomposition mechanism of the complex was studied by using differential scanning calorimetry (DSC), thermogravimetry-derivative thermogravimetry (TG-DTG) and FT-IR techniques. Results show that the final residue of thermal decomposition at 500 °C is MnO.

**Key words:** physical chemistry; manganese (II); carbohydrazide; azido complex; crystal structure; thermal decomposition mechanism

**CLC number:** TJ55; O741+.6; O64

**Document code:** A

### 1 Introduction

Energetic materials chemists have paid a lot of interest in lead-free coordination complexes because of their additional advantage of being eco-friendly and high detonation velocity<sup>[1]</sup>. To obtain high explosive performance with a coordination complex, ligands must be highly energetic and rich in oxygen and nitrogen content, such as energetic heterocyclic ligands based on tetrazoles<sup>[2]</sup> and triazoles<sup>[3]</sup>, high nitrogen catenulate ligands including hydrazium<sup>[4-5]</sup>, carbohydrazide (CHZ)<sup>[6]</sup> and so on. Carbohydrazide is an interesting azotic ligand with non-bonded lone pair of electrons on the nitrogen of amino group and oxygen of the carbonyl group. ZHANG Tong-lai et al<sup>[7]</sup> have studied the molecular structure and physicochemical properties of cadmium carbohydrazide perchlorate (GTG): a potential primary explosive. The synthesis and characterization of the transition metal nitrate as well as perchlorate complexes with carbo-

hydrazide and metal azide complexes with carbohydrazide have been reported by Sindistkii et al<sup>[8-9]</sup>. Moreover, a lot of interests have been shown in the studies of azido ions in recent years, mainly due to their explosive nature, ability to form pure and mixed ligand complexes, their ambidentate nature and bridging capacity<sup>[10-12]</sup>. The synthesis and study of energetic, low-toxic and environmentally friendly energetic complexes for possible military application has been a long term goal in our research group<sup>[7,13]</sup>. In this paper, in order to deepen the studies on the metal azide complex with carbohydrazide, the energetic complex  $\text{Mn}(\text{CHZ})_2(\text{N}_3)_2$  was synthesized, and its crystal structure and the thermal decomposition were also studied.

### 2 Experimental

#### 2.1 Materials and methods

The starting material, carbohydrazide, was synthesized by refluxing diethyl carbonate with hydrazine hydrate following the reported procedure<sup>[14]</sup> and was recrystallised before its use in the synthesis. All other chemicals were of A. R. grade chemicals and used without further purification as commercially obtained.

#### 2.2 Synthesis of $\text{Mn}(\text{CHZ})_2(\text{N}_3)_2$

A solution containing carbohydrazide (1.82 g,

**Received Date:** 2008-04-02; **Revised Date:** 2008-07-02

**Project Supported:** NSAF Foundation (No. 10776002) of the National Natural Science Foundation of China (NSFC) and Chinese Academy of Engineering Physics (CAEP)

Corresponding Author: ZHANG Tong-lai (1960 -), male, research fields: energetic materials. e-mail: ztlbit@bit.edu.cn

0.02 mol) in 18 mL of distilled water was charged into a glass reactor with a water bath. It was kept under mechanical stirring and heated to the temperature of 60 °C. 2.45 g (0.01 mol) of manganese acetate tetrahydrate dissolved in 25 mL of distilled water was added to the carbonylhydrazide solution over a period of 10 min with continuous stirring at 60 °C. The mixture was stirred for 5 min, and then a solution of sodium azide (1.3 g, 0.02 mol) dissolved in 13 mL of distilled water was added slowly with constant stirring. The solution was stirred for an additional 15 min at 60 °C and then cooled to room temperature. The resultant faint yellow mixture was filtered and kept undisturbed at room temperature, and faint yellow quadrate single crystals suitable for X-ray analysis were obtained after three days. The crystals were filtered and washed with methanol and dried in vacuum. Yield: 2.01 g (63%, based on manganese). IR (cm<sup>-1</sup>, KBr pellets): 3317s ( $\nu_{\text{as}} \text{NH}_2$ ), 3263s ( $\nu_{\text{s}} \text{NH}_2$ ), 2084vs ( $\nu_{\text{as}} \text{N}_3$ ), 2053vs ( $\nu_{\text{as}} \text{N}_3$ ), 1644vs ( $\nu \text{C}=\text{O}$ ), 1517s ( $\delta \text{NH}_2$ ), 1342w ( $\nu_{\text{s}} \text{N}_3$ ), 977w ( $\nu \text{N}-\text{N}$ ), 521w ( $\delta \text{N}_3$ ). Elemental analysis for C<sub>2</sub>H<sub>12</sub>N<sub>14</sub>O<sub>2</sub>Mn (molar mass: 319.2 g · mol<sup>-1</sup>) (%): calculated C 7.53; H 3.79; N 61.43; found C 7.41; H 3.81; N 61.50.

### 2.3 X-ray data collection and structure refinement

A paint yellow quadrate single crystal with dimensions of 0.30 mm × 0.24 mm × 0.18 mm was selected for X-ray diffraction analysis. The data collection was performed on a Bruker SMART 1000 CCD area detector diffractometer with graphite monochromated Mo K<sub>α</sub> radiation ( $\lambda = 0.71073 \text{ \AA}$ ) at 293(2) K with phi and omega scans mode. A total of 3175 reflections (2138 unique,  $R_{\text{int}} = 0.0181$ ) were measured in the range of  $2.31^\circ < \theta < 25.02^\circ$ , of which 1943 were observed with  $I > 2\sigma(I)$ . The scaled maximum and minimum transmission factors are 1.000 and 0.753, respectively. A semi-empirical absorption correction (SADABS) was applied to the raw intensities<sup>[15]</sup>. The structure was solved by direct methods using SHELXS-97 program<sup>[16]</sup> and refined by full-matrix least-squares methods on  $F^2$  with SHELXL-97 program<sup>[17]</sup>. All non-hydrogen atoms were obtained from the difference Fourier map and refined anisotropically. The hydrogen atoms were obtained geometrically and treated by a constrained refinement. The detailed crystallographic data are listed in Table 1.

**Table 1** Crystal data and structure refinement parameters for Mn(CHZ)<sub>2</sub>(N<sub>3</sub>)<sub>2</sub>

CCDC No.	665712
empirical formula	C <sub>2</sub> H <sub>12</sub> N <sub>14</sub> O <sub>2</sub> Mn
molar mass/g · mol <sup>-1</sup>	319.20
temperature/K	293(2)
crystal system	triclinic
space group	<i>P</i> $\bar{1}$
crystal size/mm	0.30 × 0.24 × 0.18
unit cell dimensions	
<i>a</i> /Å	8.2217(17)
<i>b</i> /Å	8.7427(18)
<i>c</i> /Å	9.4532(19)
$\alpha$ (°)	86.376(4)
$\beta$ (°)	69.104(3)
$\gamma$ (°)	74.019(3)
<i>V</i> /Å <sup>3</sup>	609.8(2)
<i>Z</i>	2
<i>h</i>	-9 ≤ <i>h</i> ≤ 9
<i>k</i>	-10 ≤ <i>k</i> ≤ 9
<i>l</i>	-11 ≤ <i>l</i> ≤ 6
<i>D<sub>c</sub></i> /g · cm <sup>-3</sup>	1.738
$\lambda$ /Å	0.71073
$\mu$ (Mo K <sub>α</sub> )/mm <sup>-1</sup>	1.112
<i>F</i> (0 0 0)	326
$\theta$ (°)	2.31-25.02
measured reflections	3175
unique data ( <i>R</i> <sub>int</sub> )	2138 (0.0181)
<i>R</i> <sub>1</sub> , <i>wR</i> <sub>2</sub> <sup>[1]</sup> [ <i>I</i> > 2σ( <i>I</i> )]	0.0316, 0.0826
<i>R</i> <sub>1</sub> , <i>wR</i> <sub>2</sub> <sup>[1]</sup> (all data)	0.0355, 0.0855
goodness-of-fit	1.132
$\delta\rho_{\text{max}}$ , $\delta\rho_{\text{min}}$ /(e/Å <sup>3</sup> )	0.450, -0.323

Note: 1)  $w = 1/[\sigma^2(F_0^2) + (0.0384P)^2 + 0.3390P]$ , where  $P = (F_0^2 + 2F_c^2)/3$ .

### 2.4 Physical techniques

Elemental analyses were performed on a Flash EA 1112 full-automatic trace element analyzer. The FT-IR spectra were recorded on a Bruker Equinox 55 infrared spectrometer (KBr pellets) in the range of 4000–400 cm<sup>-1</sup> with the resolution of 4 cm<sup>-1</sup>. DSC and TG measurements were carried out using Pyris-1 differential scanning calorimeter and Pyris-1 thermogravimetric analyzer (Perkin Elmer, USA), respectively, using dry nitrogen as atmosphere with flowing rate of 20 mL · min<sup>-1</sup>. The conditions for the thermal analyses were as follows: for Pyris-1 DSC, the crystal sample was powdered and sealed in aluminum pans with a linear heating rate of 10 °C · min<sup>-1</sup> from 50 °C to 500 °C; for Pyris-1 TGA, the crystal sample was powdered and put in the platinum open pans with heating rate of 10 °C · min<sup>-1</sup> from 50 °C to 500 °C.

### 3 Results and discussion

#### 3.1 Molecular structure

A perspective view of the title compound is shown in Fig. 1 and the selected bond distances and angles are listed in Table 2. The isolated manganese(II) cation exhibits a highly distorted-octahedral coordination sphere with two nitrogen atoms (N(9), N(12)) of the two terminal azido ligands and two oxygen atoms (O(1), O(2)) of the two bidentate carbohydrazide ligands forming the equatorial plane. The nitrogen atom of one carbohydrazide ligand (N(1)) and the nitrogen atom of the other carbohydrazide ligand (N(5)) are situated in the axial positions. The manganese(II) ion deviates 0.0582 Å from the average equatorial plane. The rather small bite angles [ $\text{N}(5)\text{—Mn}(1)\text{—O}(2)$ ,  $\text{N}(1)\text{—Mn}(1)\text{—O}(1)$ : 72.51(7), 72.24(6)°] of the two bidentate carbohydrazide ligands and the small bond angle of  $\text{N}(1)\text{—Mn}(1)\text{—N}(5)$  (148.28(7)°) along the axial position cause the largest distortion of the geometry. The two bidentate carbohydrazide ligands are arranged cis, whereas the structure of the title complex reveal *cis-trans-cis* arrangement in the sequence of *cis*- $\text{Mn}(\text{N}(\text{azido}))_2$ , *trans*- $\text{Mn}(\text{N}(\text{CHZ}))_2$  and *cis*- $\text{Mn}(\text{O}(\text{CHZ}))_2$ . Conforming to the general characters of coordinated azides<sup>[18]</sup>, the two terminal azido ligands are linear [ $\text{N}(9)\text{—N}(10)\text{—N}(11)$ ,  $\text{N}(12)\text{—N}(13)\text{—N}(14)$ : 178.3(4), 179.1(3)°] within experimental error and one of the azide ligands shows asymmetric N—N distances [ $\text{N}(9)\text{—N}(10)$ ,  $\text{N}(10)\text{—N}(11)$ : 1.125(4), 1.149(4) Å], while the other is essentially symmetric [ $\text{N}(12)\text{—N}(13)$ ,  $\text{N}(13)\text{—N}(14)$ : 1.170(3), 1.166(3) Å]. The average

$\text{Mn—N}_{\text{azide}}$  bond distances are comparable with those reported<sup>[19–20]</sup> which contain terminal azido ligands, but the  $\text{Mn—N}_\alpha\text{—N}_\beta$  bond angles at 146.7(3)° [ $\text{Mn}(1)\text{—N}(9)\text{—N}(10)$ ] and 126.0(2)° [ $\text{Mn}(1)\text{—N}(12)\text{—N}(13)$ ] differ significantly. This accounts for the observation of two  $\nu_{\text{as}}(\text{N}_3)$  stretching frequencies of equal intensity in the infrared spectrum of the title complex.

Carbohydrazide acts as bidentate ligand through the carbonyl oxygen atom and one of the terminal nitrogen atoms and thus forming two steady five-membered chelate rings with central manganese(II) ion. All the non-hydrogen atoms of each five-membered chelate rings is quasi-coplanar and the dihedral angle between two planes is 79.254° indicating that the two planes are quasi-vertical which reducing the steric hindrance and enhancing the toughness and stability of the molecule of  $\text{Mn}(\text{CHZ})_2(\text{N}_3)_2$ . The average bond distances of  $\text{Mn—N}_{\text{CHZ}}$  (2.283 Å) and  $\text{Mn—O}_{\text{CHZ}}$  (2.243 Å) are comparable with reported data in [ $\text{Mn}(\text{CHZ})_3(\text{ClO}_4)_2$  ( $\text{Mn—N}_{\text{CHZ}}$ , 2.295 Å;  $\text{Mn—O}_{\text{CHZ}}$ , 2.149 Å)<sup>[21]</sup>.

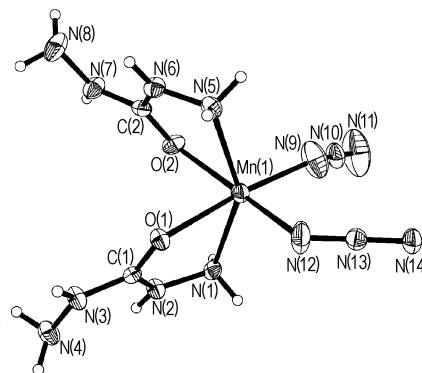


Fig. 1 Molecular structure of  $\text{Mn}(\text{CHZ})_2(\text{N}_3)_2$  (ellipsoids are drawn at the 30% probability level)

Table 2 Selected bond lengths and bond angles

bond	distance/Å	bond	distance/Å	bond	distance/Å
$\text{Mn}(1)\text{—N}(9)$	2.118(3)	$\text{O}(2)\text{—C}(2)$	1.260(3)	$\text{N}(7)\text{—C}(2)$	1.327(3)
$\text{Mn}(1)\text{—N}(12)$	2.176(3)	$\text{N}(1)\text{—N}(2)$	1.412(3)	$\text{N}(7)\text{—N}(8)$	1.409(3)
$\text{Mn}(1)\text{—O}(2)$	2.2330(17)	$\text{N}(2)\text{—C}(1)$	1.348(3)	$\text{N}(9)\text{—N}(10)$	1.125(4)
$\text{Mn}(1)\text{—O}(1)$	2.2527(16)	$\text{N}(3)\text{—C}(1)$	1.330(3)	$\text{N}(10)\text{—N}(11)$	1.149(4)
$\text{Mn}(1)\text{—N}(1)$	2.282(2)	$\text{N}(3)\text{—N}(4)$	1.413(3)	$\text{N}(12)\text{—N}(13)$	1.170(3)
$\text{Mn}(1)\text{—N}(5)$	2.284(2)	$\text{N}(5)\text{—N}(6)$	1.410(3)	$\text{N}(13)\text{—N}(14)$	1.166(3)
$\text{O}(1)\text{—C}(1)$	1.253(3)	$\text{N}(6)\text{—C}(2)$	1.342(3)		
bond	angle/(°)	bond	angle/(°)	bond	angle/(°)
$\text{N}(9)\text{—Mn}(1)\text{—N}(12)$	90.06(12)	$\text{N}(12)\text{—Mn}(1)\text{—N}(1)$	101.74(10)	$\text{N}(1)\text{—Mn}(1)\text{—N}(5)$	148.28(7)
$\text{N}(9)\text{—Mn}(1)\text{—O}(2)$	97.84(11)	$\text{O}(2)\text{—Mn}(1)\text{—N}(1)$	85.17(7)	$\text{N}(10)\text{—N}(9)\text{—Mn}(1)$	146.7(3)
$\text{N}(12)\text{—Mn}(1)\text{—O}(2)$	167.87(9)	$\text{O}(1)\text{—Mn}(1)\text{—N}(1)$	72.24(6)	$\text{N}(9)\text{—N}(10)\text{—N}(11)$	178.3(4)
$\text{N}(9)\text{—Mn}(1)\text{—O}(1)$	174.60(12)	$\text{N}(9)\text{—Mn}(1)\text{—N}(5)$	100.33(12)	$\text{N}(13)\text{—N}(12)\text{—Mn}(1)$	126.0(2)
$\text{N}(12)\text{—Mn}(1)\text{—O}(1)$	86.11(8)	$\text{N}(12)\text{—Mn}(1)\text{—N}(5)$	97.09(10)	$\text{N}(14)\text{—N}(13)\text{—N}(12)$	179.1(3)
$\text{O}(2)\text{—Mn}(1)\text{—O}(1)$	86.56(7)	$\text{O}(2)\text{—Mn}(1)\text{—N}(5)$	72.51(7)		
$\text{N}(9)\text{—Mn}(1)\text{—N}(1)$	104.90(11)	$\text{O}(1)\text{—Mn}(1)\text{—N}(5)$	83.94(7)		

As shown in Fig. 2, there are two types of weak intermolecular hydrogen bonds among  $\text{Mn}(\text{CHZ})_2(\text{N}_3)_2$  molecules. One occurs between carbohydrazide ligands and end nitrogen atoms of azide groups of adjacent complex molecules [ $\text{N}(1)-\text{H}(1\text{B})\cdots\text{N}(14)\#1$ ,  $\text{N}(3)-\text{H}(3)\cdots\text{N}(14)\#3$ ,  $\text{N}(7)-\text{H}(7)\cdots\text{N}(14)\#5$ ]. The other forms an  $\text{N}-\text{H}\cdots\text{O}$  hydrogen bond [ $\text{N}(2)-\text{H}(2)\cdots\text{O}(2)\#2$ ,  $\text{N}(6)-\text{H}(6)\cdots\text{O}(1)\#4$ ] which occurs between two carbohydrazide ligands of adjacent complex molecules. The hydrogen bond distances and angles are summarized in Table 3. All of these intermolecular hydrogen bonds extend the structure into a 3D supramolecular array and make an important contribution to enhance the thermal stability of the title complex.

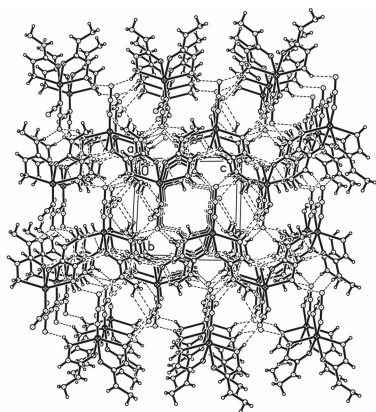


Fig. 2 Packing plot of  $\text{Mn}(\text{CHZ})_2(\text{N}_3)_2$  along a-axis of unit cell, broken lines indicate hydrogen bonds

Table 3 Hydrogen bond lengths and bond angles

D—H...A	d(D—H) /Å	d(H...A) /Å	d(D...A) /Å	∠DHA /(°)
N(1)—H(1B)⋯N(14) #1	0.9000	2.2300	3.050(3)	151.00
N(2)—H(2)⋯O(2) #2	0.8600	2.1600	2.943(3)	151.00
N(3)—H(3)⋯N(14) #3	0.8600	2.2200	3.072(3)	168.00
N(6)—H(6)⋯O(1) #4	0.8600	2.1100	2.907(3)	153.00
N(7)—H(7)⋯N(14) #5	0.8600	2.2000	3.049(4)	167.00

Note: Symmetry codes: #1  $-x+1, -y+1, -z+2$ ; #2  $-x, -y+2, -z+2$ ; #3  $x, y+1, z$ ; #4  $-x+1, -y+2, -z+1$ ; #5  $x-1, y+1, z$

### 3.2 Thermal decomposition mechanism

The DSC and TG-DTG curves under the linear heating rate of  $10\text{ }^\circ\text{C}\cdot\text{min}^{-1}$  with nitrogen atmosphere are shown in Fig. 3 and Fig. 4 to demonstrate the thermal decomposition processes of  $\text{Mn}(\text{CHZ})_2(\text{N}_3)_2$ . In the DSC curve, the endothermic peak starts at  $159\text{ }^\circ\text{C}$ , ends at  $191\text{ }^\circ\text{C}$ , and the peak temperature is  $181\text{ }^\circ\text{C}$ . The enthalpy of this endothermic process is  $38.21\text{ kJ}\cdot\text{mol}^{-1}$ . The

TG-DTG curves show that there is no mass loss corresponding to this temperature range and the IR spectrum of the solid residue at  $195\text{ }^\circ\text{C}$  is very similar to that of  $\text{Mn}(\text{CHZ})_2(\text{N}_3)_2$ , which indicates that this endothermic process is the melting process of the sample. The peak temperatures and enthalpies of the two exothermic processes are as follows:  $247\text{ }^\circ\text{C}$  ( $209-272\text{ }^\circ\text{C}$ ) and  $86.02\text{ kJ}\cdot\text{mol}^{-1}$ ,  $293\text{ }^\circ\text{C}$  ( $272-306\text{ }^\circ\text{C}$ ) and  $630.76\text{ kJ}\cdot\text{mol}^{-1}$ .

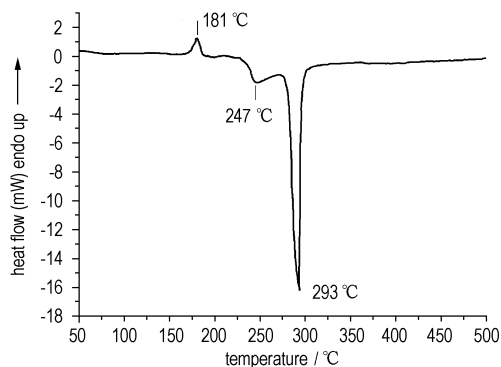


Fig. 3 The DSC curve of  $\text{Mn}(\text{CHZ})_2(\text{N}_3)_2$

under  $\text{N}_2$  atmosphere with a heating rate of  $10\text{ }^\circ\text{C}\cdot\text{min}^{-1}$

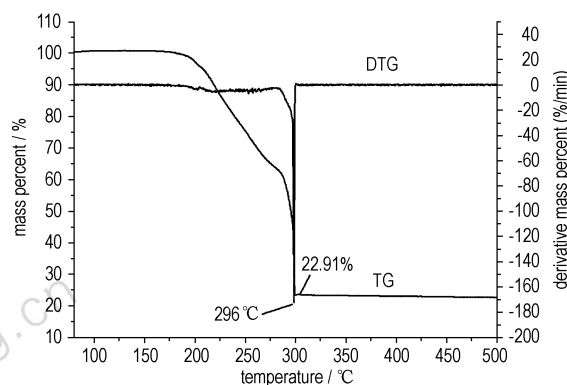


Fig. 4 The TG-DTG curves of  $\text{Mn}(\text{CHZ})_2(\text{N}_3)_2$

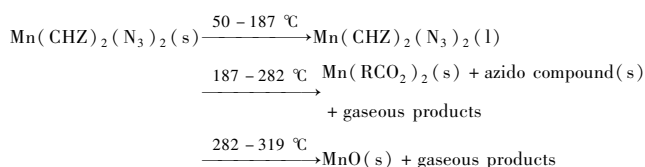
under  $\text{N}_2$  atmosphere with a heating rate of  $10\text{ }^\circ\text{C}\cdot\text{min}^{-1}$

In the TG-DTG curves, there are two main successive mass loss stages from  $50$  to  $500\text{ }^\circ\text{C}$ , which corresponds to the two exothermic processes in the DSC curve. The first mass loss stage starts at  $187\text{ }^\circ\text{C}$ , ends at  $282\text{ }^\circ\text{C}$ , and reaches the largest rate at  $252\text{ }^\circ\text{C}$  with mass loss percentage of  $36.33\%$  of the initial weight. The thermal decomposition process and the breaking-up of the chelate rings are confirmed from the FT-IR spectrum of the solid residue at  $285\text{ }^\circ\text{C}$ . The disappearances of the characteristic absorption of  $\text{NH}_2$  at  $3317, 3263, 1517, 1187\text{ cm}^{-1}$  account for the breaking of two chelate rings and the part-

ly decomposition of two carbohydrazide ligands. The new absorption peaks at 1633, 1561, 1400  $\text{cm}^{-1}$  are assigned to  $\text{RCO}_2^-$  in the solid residue<sup>[22-23]</sup>. However, the absorption at 2075  $\text{cm}^{-1}$  indicates that the azido ligands of the complex still exist.

The second stage with the larger mass loss percentage of 40.70% at 296 °C starts at 282 °C and ends at 319 °C. This stage is predicted as the decomposition of azido ligands and  $\text{RCO}_2^-$  as well as the formation of MnO (Found 22.91%, calcd. 22.22%). The disappearance of all the characteristic absorption bands of  $\text{Mn}(\text{CHZ})_2(\text{N}_3)_2$  and the existence of the absorption peak at 606, 531  $\text{cm}^{-1}$  in the FT-IR spectrum of the final residue at 500 °C also prove that the final residue is MnO.

In conclusion, on the basis of the DSC, TG-DTG and FT-IR analyses, the thermal decomposition processes of  $\text{Mn}(\text{CHZ})_2(\text{N}_3)_2$  are predicted as follows:



## 4 Conclusion

In the title complex,  $\text{N}_3^-$  acts as monodentate ligand, whereas carbohydrazide serves as bidentate ligand through the carbonyl oxygen atom and one of the terminal nitrogen atoms. As a result, the central manganese (II) cation exhibits a highly distorted-octahedral coordination sphere. The net structure of a 3D supramolecular array is formed through coordination bonds and hydrogen bonds. The thermal decomposition mechanism of the title complex shows that it has better thermal stability, and it can be further studied in potential use for initiator.

### References:

- [1] Huynh M H V, Hiskey M A, Meyer T J, et al. Green primaries; Environmentally friendly energetic complexes[J]. *Proceedings of the National Academy of Sciences of the United States of America*, 2006, 103(14): 5409-5412.
- [2] Huynh M H V, Coburn M D, Meyer T J, et al. Green primary explosives; 5-Nitrotetrazolato- $\text{N}_2$ -ferrate hierarchies[J]. *Proceedings of the National Academy of Sciences of the United States of America*, 2006, 103(27): 10322-10327.
- [3] ZHANG Tong-lai, HU Rong-zu, LIANG Yan-jun, et al. Preparation and mechanism of thermal decomposition of alkalimetal (Li, Na and K) salts of 3-nitro-1,2,4-triazol-5-one [J]. *Journal of Thermal Analysis*, 1993, 39: 827-847.
- [4] Chhabra J S, Talawar M B, Makashir P S, et al. Synthesis, characterization and thermal studies of (Ni/Co) metal salts of hydrazine; Potential initiatory compounds[J]. *Journal of Hazardous Materials*, 2003, A99(3): 225-239.
- [5] ZHU Shun-guan, WU You-cheng, ZHANG Wen-yi, et al. Evaluation of a new primary explosive; nickel hydrazine nitrate (NHN) complex [J]. *Propellants Explosives Pyrotechnics*, 1997, 22(6): 317-320.
- [6] Talawar M B, Agrawal A P, Chhabra J S, et al. Studies on lead-free initiators; synthesis, characterization and performance evaluation of transition metal complexes of carbohydrazide [J]. *Journal of Hazardous Materials*, 2004, A113(1-3): 57-65.
- [7] ZHANG Tong-lai, WEI Zhao-rong, Lü Chun-hua, et al. Research on the primary explosive GTG [J]. *Explosive Materials (Baopo Qicai)*, 1999, 28(3): 16-19.
- [8] Sinditskii V P, Fogelzang A E, Dutov M D, et al. Structure of transition metal chloride, sulgate, nitrate and perchlorate complexes with carbohydrazine [J]. *Russian Journal of Inorganic Chemistry*, 1987, 32(8): 1944-1949.
- [9] Sinditskii V P, Vernidub T Y, Fogelzang A E. Metal azide complexes with carbohydrazide [J]. *Russian Journal of Inorganic Chemistry*, 1990, 35(3): 685-688.
- [10] SHENG Di-lun, MA Feng-e. Synthesis and main properties of new initiating explosive DACP [J]. *Chinese Journal of Energetic Materials (Hanneng Cailiao)*, 2006, 14(3): 161-164.
- [11] Hammerl A, Holl G, Kaiser M, et al. New hydrazinium azide compounds [J]. *Zeitschrift für Anorganische und Allgemeine Chemie*, 2001, 627: 1477-1482.
- [12] Patil K C, Nesamani C, Verneker V R P. Synthesis and characterisation of metal hydrazine nitrate, azide and perchlorate complexes [J]. *Synthesis and Reactivity in Inorganic and Metal-Organic Chemistry*, 1982, 12(4): 383-395.
- [13] ZHANG Tong-lai, Lü Chun-hua, ZHANG Jian-guo. Preparation and molecular structure of  $\{[\text{Ca}(\text{CHZ})_2(\text{H}_2\text{O})](\text{NTO})_2 \cdot 3.5\text{H}_2\text{O}\}_n$  [J]. *Propellants Explosives Pyrotechnics*, 2003, 28(5): 271-276.
- [14] WEI Zhao-rong. Studies on carbohydrazine and energetic complexes with carbohydrazine [D]. Beijing: Beijing Institute of Technology, 1998.
- [15] Sheldrick G M. SADABS; Program for empirical absorption correction of area detector data [CP]. Germany: University of Göttingen, 1996.
- [16] Sheldrick G M. SHELXS-97, Program for the solution of crystal structures [CP]. Germany: University of Göttingen, 1997.
- [17] Sheldrick G M. SHELXL-97, Program for the refinement of crystal structures [CP]. Germany: University of Göttingen, 1997.
- [18] Dori Z, Ziolo R F. The chemistry of coordinated azides [J]. *Chemical Reviews*, 1973, 73(3): 247-254.
- [19] Cortés R, Pizarro J L, Lezama L, et al. Ferromagnetic interactions in the first bis( $\mu$ -end-on-azido) manganese(II) dinuclear compound:  $[\text{Mn}(\text{terpy})(\text{N}_3)_2]_2 \cdot 2\text{H}_2\text{O}$  [J]. *Inorganic Chemistry*, 1994, 33(12): 2697-2700.

- [20] Das D, Chand B G, Wu J S, et al. Manganese(II)-azido/thiocyanato complexes of naphthylazoimidazoles: X-ray structures of  $\text{Mn}(\beta\text{-NaiEt})(\text{X})_2$  ( $\beta\text{-NaiEt}$  = 1-ethyl-2-(naphthyl- $\beta$ -azo)imidazole;  $\text{X} = \text{N}_3^-$ ,  $\text{NCS}^-$ ) [J]. *Journal of Molecular Structure*, 2007, 842 (1-3): 17-23.
- [21] ZHANG Jian-guo, ZHANG Tong-lai, WEI Zhao-rong, et al. Studies on preparation, crystal structure and application of  $[\text{Mn}(\text{CHZ})_3](\text{ClO}_4)_2$  [J]. *Chemical Journal of Chinese Universities*, 2001, 22 (6): 895-897.
- [22] LI Yu-feng, ZHANG Tong-lai, ZHANG Jian-guo, et al. Preparation, crystal structure and thermal decomposition mechanism of  $[\text{K}(\text{HTNR})(\text{H}_2\text{O})]_n$  [J]. *Acta Chimica Sinica*, 2003, 61(7): 1020-1024.
- [23] CHEN Hong-yan, ZHANG Tong-lai, ZHANG Jian-guo, et al. Crystal structure, thermal decomposition and properties of cesium 3,5-dihydroxy-2,4,6-trinitrophenolate [J]. *Propellants Explosives Pyrotechnics*, 2006, 31(4): 285-289.

## Mn(CHZ)<sub>2</sub>(N<sub>3</sub>)<sub>2</sub> 配合物的合成、晶体结构与热分解研究

刘振华, 张同来, 张建国, 杨利, 张进, 臧艳

(北京理工大学爆炸科学与技术国家重点实验室, 北京 100081)

**摘要:** 合成了以碳酰肼(CHZ)为配体,以叠氮离子为混合配体的配合物:  $\text{Mn}(\text{CHZ})_2(\text{N}_3)_2$ , 并对其进行了元素分析及红外表征。利用X射线单晶分析测定了其晶体结构,晶体属于三斜晶系,  $P\bar{1}$  空间群,晶体学数据为:  $a = 8.2217(17) \text{ \AA}$ ,  $b = 8.7427(18) \text{ \AA}$ ,  $c = 9.4532(19) \text{ \AA}$ ,  $\alpha = 86.376(4)^\circ$ ,  $\beta = 69.104(3)^\circ$ ,  $\gamma = 74.019(3)^\circ$ ,  $V = 609.8(2) \text{ \AA}^3$ ,  $D_c = 1.738 \text{ g} \cdot \text{cm}^{-3}$ ,  $Z = 2$ ,  $R_1 = 0.0316$ ,  $wR_2[I > 2\sigma(I)] = 0.0826$ ,  $S = 1.132$ 。中心 Mn(II) 离子与两个碳酰肼分子和两个叠氮离子配位形成六配位八面体结构,其中碳酰肼分子通过羰基上的氧原子和端基上的氮原子以二齿螯合配体方式配位,叠氮离子通过端基氮原子以单齿配体方式配位。用 DSC、TG-DTG 技术研究了标题配合物的热分解,研究表明,在 500 °C, 分解的最终残渣为 MnO。

**关键词:** 物理化学; 锰(II); 碳酰肼; 叠氮配合物; 晶体结构; 热分解机理

中图分类号: TJ55; O741+.6; O64

文献标识码: A

(上接 651 页)

- [19] XU Xiao-juan, XIAO He-ming, GONG Xue-dong, et al. Theoretical studies on the vibrational spectra, thermodynamic properties, detonation properties, and pyrolysis mechanisms for polynitroadamantanes [J]. *J Phys Chem A*, 2005, 109: 11268-11274.
- [20] David R L. CRC Handbook of Chemistry and Physics [M]. LLC: CRC Press 2005.
- [21] Rice B M, Pai S V, Hare J. Predicting heats of formation of energetic materials using quantum mechanical calculations [J]. *Combustion and Flame*, 1999, 118: 445-458.

## Heats of Formation for Energetic Compounds Calculated using Atomization Reactions

QIU Li-mei<sup>1,2</sup>, GONG Xue-dong<sup>1</sup>, ZHENG Jian<sup>2</sup>, XIAO He-ming<sup>1</sup>

(1. Computation Research Institute of Molecules and Materials, Department of Chemistry, Nanjing University of Science and Technology, Nanjing 210094, China;

2. The 42nd Institute of the Fourth Academy of China Aerospace Science and Technology, Xiangfan 441003, China)

**Abstract:** Based on the calculated results at DFT-B3LYP/6-31G\* or HF/6-31G\* level, heats of formation for 49 energetic compounds were calculated using atomization reactions and physical chemistry equation. By comparing the theoretical and experimental results, a good linear correlation between the experimental heats of formation ( $y$ ) and the ones calculated at B3LYP/6-31G\* level ( $x$ ) is obtained. For the investigated energetic compounds, the linear equation, the correlative coefficient and the standard deviation are  $y = -75.79 + 0.98x$ , 0.990 and 28.21, respectively. Heats of formation obtained by using the linear equation are close to the experimental ones. The results show that by means of atomization reactions and using the results of B3LYP/6-31G\* calculation, heats of formation for energetic materials can be obtained. In comparison, the same method based on the results at HF/6-31G\* level is not fit for calculating the heats of formation for energetic compounds.

**Key words:** physical chemistry; heat of formation; energetic compound; density functional theory (DFT); atomization reaction